Mem. S.A.It. Vol. 76, 441

Memorie della

AGB and post-AGB stars

Dieter Engels

Hamburger Sternwarte, Gojenbergsweg 112, D-21029 Hamburg, Germany
e-mail: dengels@hs.uni-hamburg.de

Abstract. Intermediate mass stars (1-8 $M_{\odot}$) evolve along the Asymptotic Giant Branch after completion of hydrogen and helium core burning. At the tip they lose for several ten to hundred thousand years copious amounts of mass and exhibit various forms of variability, as for example large-amplitude variations with periods of one to five years. In the oxygen-rich circumstellar envelopes powerful OH, H_2O and SiO masers may operate. Part of the AGB population is converted to carbon stars. During the latest phases of AGB evolution the mass loss rates approach several 10^{-5} $M_{\odot}$ yr^{-1}, so that the stars become invisible in the optical and in part in the near infrared.
On departure from the AGB a fundamental transition in the mass loss process is taking place changing from a spherically symmetric outflow on the AGB to axi-symmetric or point-symmetric geometries. While the mass loss rates decrease to $\approx 10^{-8}$ $M_{\odot}$ yr^{-1}, the velocities are strongly increasing. Stars are now in their "post-AGB" phase. Mounting evidence is gathered that during the very latest phase of AGB evolution and during the post-AGB phase, evolution proceeds on very short timescales, which in extreme cases is comparable to the working life of an astronomer.

Key words. Stars: AGB and post-AGB

1. Introduction

The time a star spends during its evolution on the Asymptotic Giant Branch (AGB) is only a tiny fraction of $\leq$1% of its total lifetime. Nevertheless this evolutionary phase sets the framework for the later development into *stellar end products* like planetary nebulae and white dwarfs. AGB stars are cool red giants and reach their maximum luminosity during the AGB phase, making them easily observable beacons in the sky. Strong infrared radiation, and in part large-amplitude variability and masers allow their efficient identification. The processes involved in the departure from the AGB are still badly understood, because the stars are dust-enshrouded and inaccessible to direct view. As post-AGB stars, they increase their temperature at almost constant luminosity, until they are able to ionize the remnant shell, creating one of the most fascinating phenomena in the sky: planetary nebulae.

The purpose of the current review is an introduction to the non-expert reader, covering the main observational properties of AGB and post-AGB stars and the current understanding of the evolutionary processes. References to further reading are given at the appropriate places. A comprehensive coverage of the field is given by the book *Asymptotic Giant Branch stars* edited by Habing & Olofsson (2004).

Send offprint requests to: D. Engels

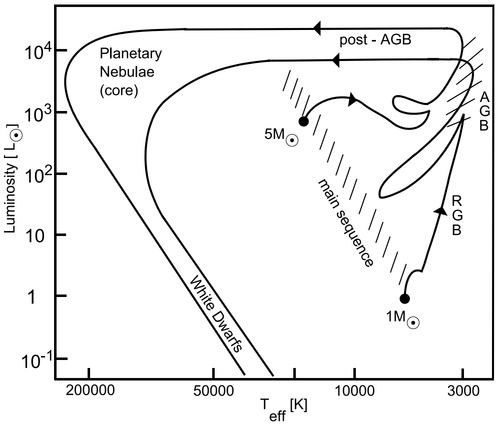

Fig. 1. Schematic evolutionary tracks of stars with main-sequence masses of 1 and 5 $M_\odot$ and solar composition. RGB = Red Giant Branch, AGB = Asymptotic Giant Branch.

2. Evolution on the AGB

Stars enter the AGB when energy production in a double shell structure begins, which is made up of an inner burning He shell surrounding an electron degenerated carbon-oxygen (C-O) core and an outer hydrogen burning shell. The stars then already have left the main sequence and have passed through the red giant branch (RGB), where energy had been generated by hydrogen fusion in a shell around a core made up of helium. The stars have completed also the core helium burning phase in which the build-up of the C-O core had started. On the AGB, double-shell burning starts with a quiescent burning phase (the E(arly)-AGB) and develops later in the thermal pulse phase (TP-AGB). The thermal pulses are large energy releases generated by a flash-like burning of the helium shell lasting several hundred years. Typical evolutionary tracks in the Hertzsprung-Russell-Diagram (HRD) are shown in Fig. 1.

The evolutionary time scales on the AGB are short compared to the main sequence lifetimes. For 1–5 $M_\odot$ stars the E-AGB phase lasts ≈1–15 million years, compared to the time spent on the main sequence of ≈0.1–12 billion years. In the TP-AGB phase stars remain another several hundred thousand years. Thus the duration of the AGB phase is 0.5% or less of the main sequence lifetime (Vassiliadis & Wood 1993, Blöcker 1995a). On the TP-AGB the stars lose most of their mass and they finally leave the AGB, when virtually only the naked C-O core is left over. The time scales derived from evolutionary models strongly depend on the adopted mass loss law. A critical review discussing the current understanding of the mechanisms leading to the strong mass loss in AGB stars and of its parameterization is discussed by Willson (2000).

3. Observational characteristics

3.1. Luminosities, masses, and chemistry

Observationally, the luminosities of AGB stars are confined to the range $-3.6 \lesssim M_{bol} \lesssim -7.1$ ($2200 \lesssim L/L_\odot \lesssim 55\,000$) and they have main-sequence masses between ≈0.85 and ≈8 $M_\odot$. The lower limits are set by AGB stars occurring in globular clusters, while the upper luminosity limit is observed for AGB stars in the Magellanic Clouds and is set by theory due to the (not strictly valid) core-luminosity relation, and the Chandrasekhar 1.4 $M_\odot$ mass limit of white dwarfs (Lattanzio & Wood 2004). The upper limit in mass is set by the observation of white dwarfs in open clusters with turn-off masses $\lesssim 8$ $M_\odot$ (Koester & Reimers 1996).

Spectroscopically, AGB stars can be divided into oxygen-rich types (spectral type M), whose spectra are dominated by TiO bands, and carbon-rich types (spectral type C), where bands of C_2 and CN dominate the spectra. The difference is due to the carbon-oxygen ratio in the atmospheres being C/O<1 for M-stars and vice versa for C-stars. Transition objects with C/O≈1 are known as S-stars. As normal stars have C/O<1, carbon stars must be enriched with extra carbon. According to AGB models, this extra carbon is brought to the surface by convection during the *third dredge-up*. This process occurs after a thermal pulse, when the convection zone is able to penetrate the hydrogen burning shell and allows to dredge-up freshly processed matter (Lattanzio & Wood 2004). A comprehensive review on carbon stars was given by Wallerstein & Knapp (1998).

3.2. Variability

As soon as the star enters the TP-AGB, the stellar emission becomes variable. It is thought that the light variations are caused by radial pulsations and additional opacity variations in the stellar atmospheres (Reid & Goldstone 2002). The most conspicuous variables having large amplitudes are the optically prominent Mira variables and the optically obscured infrared bright OH/IR stars, although irregular and semi-irregular (SR) pulsators with small amplitudes are more frequent. The periods of Mira variables are of the order ≈1 year and the visual amplitudes are large (>2.5 mag), while the periods of OH/IR stars are between 2 and 5 years and the amplitudes in the near infrared can reach a few magnitudes (Engels et al. 1983). The light curves of many Miras are sampled frequently due to the efforts of amateur observers (see www.aavso.org), but this is not the case for OH/IR stars due to the need of infrared or radio equipment.

3.3. Mass loss, circumstellar shells

The energy generating core region is surrounded by a tenuous and extended envelope in which mixing occurs by convection. The size of the envelope may easily match earth's orbit.The outer layers are bounded only weakly by gravitation so that the stars lose mass already on the E-AGB at rates ($\lesssim 10^{-7}\ M_\odot\,\mathrm{yr}^{-1}$) ten orders of magnitude higher than that of the sun.

The stellar pulsation on the TP-AGB extends the outer layers of the envelopes to cooler regions facilitating the formation of molecules and dust. Once dust has formed, radiation pressure is able to push it away dragging the gas with it. Mass loss rates increase dramatically reaching up to $10^{-4}\ M_\odot\,\mathrm{yr}^{-1}$ and the outflows reach typical velocities of $v_E = 10 - 15\ \mathrm{kms}^{-1}$.

The development of high mass loss rates leads to the formation of a circumstellar gas and dust shell (circumstellar envelope, CSE)

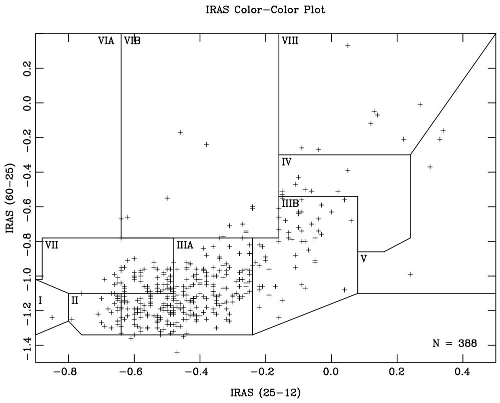

Fig. 2. IRAS color-color plot with the location of the O-rich AGB stars from the 'Arecibo sample' (Lewis 1994). The labeled regions were introduced by Van der Veen & Habing (1988). Regions I-IV contain mostly O-rich stars, VI and VII mostly C-rich stars, and V and VIII many post-AGB stars.

with increasing optical depths. (AGB CSEs have been reviewed by Habing 1996.) At rates $\gtrsim 10^{-6}\ M_\odot\,\mathrm{yr}^{-1}$ the stars disappear optically. The stellar emission is absorbed by the dust and re-emitted in the infrared. The obscured AGB stars were originally discovered by OH maser surveys and subsequent identifications in the infrared ("OH/IR stars"). Larger populations were later found by the IRAS All-Sky Survey at 10–100 μm, applying color selection criteria. They divide IRAS color-color plots into regions (Fig. 2), in which AGB stars can be separated efficiently from other objects. The distribution of OH/IR stars in Fig. 2 has the form of a sequence demonstrating the wide range of optical depths involved. The blue end of the sequence is made up by stars with optically thin CSEs (SR-, Mira variables), while the objects in the red part of the diagram have optically thick CSEs (OH/IR stars).

The dichotomy between M- and C-stars is observed also in the infrared as the chemistry of their CSEs differ according to the C/O-ratio of the outflowing matter. As carbon is locked for C/O>1 almost completely in the CO molecule, only oxygen-rich stars are able to form oxygen-bearing dust. This dust is mainly made of amorphous silicates which exhibit a very strong feature at 9.7μm in emission for

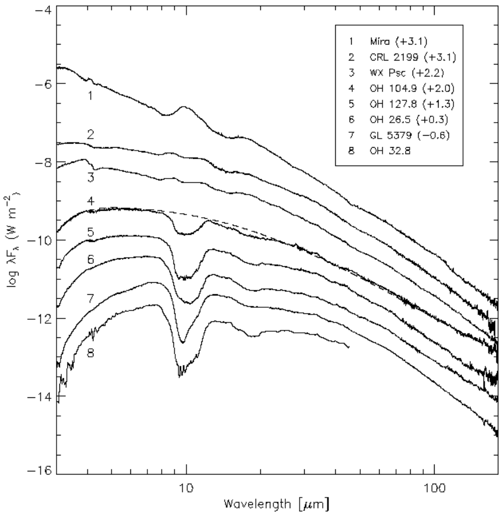

Fig. 3. ISO spectra of the 6–200μm region of several O-rich AGB stars. The spectra are shifted to order them in terms of 10μm optical depth, which correlates roughly with IRAS colors and mass loss rates (from Sylvester et al. (1999))

optically thin and in absorption for thick CSEs (Fig. 3). In contrast, the dominant dust species contained in carbon star CSEs is graphite. A classification even of obscured AGB stars discovered by IRAS was therefore possible using the dust signatures found in the spectra taken in the 10μm range by the IRAS Low Resolution Spectrometer (LRS). The knowledge of the dust constituents has tremendously increased with the detailed spectroscopy of AGB stars in the mid-infrared by the Infrared Space Observatory (ISO) (Molster & Kemper 2005, Blommaert 2005).

3.4. Masers

The CSEs, extending to sizes 10^{16} – 10^{17} cm (>1000 AU), provide ample space for velocity coherent outflow required for powerful maser emission. The emission always involves molecules containing oxygen. The most prominent are the OH masers at 1612 and 1665/1667 MHz, the H_2O maser at 22 GHz and the SiO masers at 43 and 86 GHz. Typical maser spectra are shown in Fig. 4. Extensive reviews on masers in CSEs have been written by Cohen (1989), and Elitzur (1992a, 1992b).

Maser surveys have shown that at low mass loss rates SiO and H_2O masers are more frequently detected than OH masers, while the detection rate of 1612 MHz OH masers is high at higher mass loss rates. Also the maser profiles show systematics depending on mass loss rates although they are often strongly variable in intensity. The 1612 MHz OH masers are located at radial distances $\geq 10^{16}$ cm, and propagate radially. Their profiles are double-peaked with the blue-shifted peak coming from the approaching front side of the shell and the red-shifted peak coming from the receding back side. The double-peaked profile immediately tells the expansion velocity of the shell (half the velocity difference between the peaks) and the radial velocity of the star (midpoint of the OH maser velocity interval). In the mm-wavelength range this information can be obtained also from the profiles of thermal CO emission.

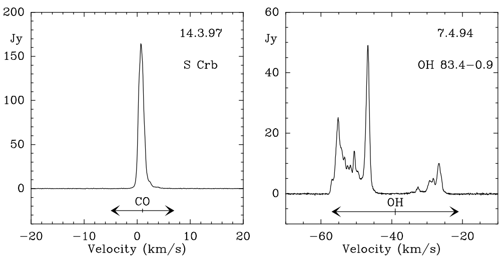

Fig. 4. H_2O maser spectra taken with the Effelsberg radio telescope. The Mira variable S Crb displays a single maser feature close to the stellar radial velocity given by the midpoint of the velocity range of the thermal CO emission. The OH/IR star OH 83.4 – 0.9 shows a double-peaked profile with a velocity range almost identical as for OH maser emission.

Because of their higher excitation temperature H_2O and SiO masers are located more inside. The SiO masers were found to be located close to the star inside the dust formation zone, while the H_2O masers are located between the SiO and OH maser zones. At lower mass loss rates these masers preferentially propagate in tangential directions, displaying maser features close to the stellar radial velocity (S Crb). In

OH/IR stars, the H_2O maser is located so far away from the star that radial amplification as in OH masers takes place: the typical double-peaked profile is displayed (OH 83.4–0.9).

Dedicated radio interferometers like the VLBA and MERLIN are nowadays used to map the distribution of maser clouds around the star and to measure proper motions. Also the strengths and distributions of magnetic fields in the CSEs can be determined by polarization measurements of the masers (Vlemmings, these proceedings). The most spectacular result so far is the monitoring of the 43 GHz SiO maser of the Mira TX Cam over a full pulsation period (Diamond & Kemball 2003). The observations revealed with bi-weekly time resolution the gas motions in the near circumstellar environment of this star. Together with the new possibilities for high-spatial resolution near-infrared imaging (see Wittkowski, these proceedings), the radio imaging of masers will allow in the coming years studies of the processes leading to the high mass loss rates observed in AGB stars in unprecedented detail.

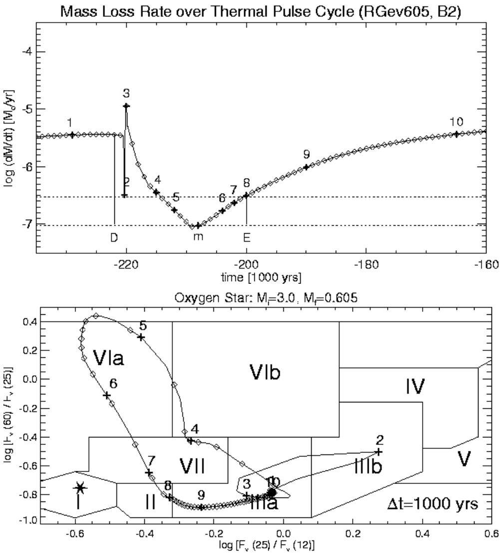

Fig. 5. Variations of the mass loss rate for one thermal pulse cycle and the correspondent location of the star in the IRAS color-color diagram of a 3 $M_\odot$ model. The separation between two adjacent diamonds corresponds to 1000 years. Labels "1" to "10" are used as reference points (from Steffen et al. 1998).

3.5. Samples

TP-AGB stars may be unambiguously identified by detection of lines of technetium in their optical spectra. Tc has only radioactive isotopes and must have been dredged-up recently. However, in general secondary criteria as the variability, the infrared excess, or the presence of masers are used as selection criteria for AGB star samples.

They can be obtained from the General Catalogue of Variable stars (Samus et al. 2004) by extracting stars classified as Miras or SR variables (Kharchenko et al. 2002). Also the carbon stars in the catalogue of Stephenson (1989) are mostly AGB stars. Statistically well described samples are easier to obtain from the IRAS Point Source Catalog applying color criteria. For example, Lewis and collaborators (Lewis 1994) provided a flux limited sample of several hundred AGB stars ('Arecibo sample'). A sample of AGB stars within 1 kpc of the sun was compiled by Jura & Kleinmann (see Olivier et al. (2001) for a recent discussion). Samples in other galaxies can be obtained using the upper luminosity limit of 2500 $L_\odot$ valid for all RGB stars (Habing 1996) as lower selection threshold. The only contamination expected is from a few red supergiants.

4. The departure from the AGB

AGB evolution ends when mass loss has removed the envelope leaving behind the C-O core. Intuitively the sequence SR⟶Mira ⟶OH/IR star of increasing mass loss rates and periods may be seen as an evolutionary sequence along the AGB to higher luminosities regardless of initial mass (Bedijn 1987). However, in response to the occurrence of thermal pulses, variations in luminosity, periods, and mass loss rates are expected and stars may cycle several times through the sequence SR⟶Mira⟶OH/IR star. As an example, Figure 5 shows variations of the mass loss rate during a single thermal pulse cycle for a 3 $M_\odot$ model (Steffen et al. 1998). As a result the spectral energy distributions (SED) and the correspondent synthetic IRAS colors will vary as well. The movement in the IRAS color-color diagram is in the form of 'loops' (Fig. 5), with their exact locations depending on chemistry and main-sequence mass. The galactic height distribution in addition is not uniform across the IRAS color-color diagram. Jiménez-Esteban (these proceedings) finds scale heights of 300–500 pc in the blue part and 100–200 pc in the red part of the color sequence, implying mass segregation. Only the more massive AGB stars may actually develop into an OH/IR star before leaving the AGB.

Part of the stars will be converted into carbon stars and leave the O-rich color sequence in the IRAS color color diagram. They may originate mainly from stars in the mass range ≈2–4 $M_{\odot}$, because the lower mass stars may not have sufficient thermal pulses and subsequent dredge-ups to invert the original C/O<1 ratio and in the higher mass stars the carbon might be quickly converted into nitrogen due to the so-called 'hot bottom burning' (Groenewegen & Marigo 2004).

Thus, stars will end their AGB evolution with different chemistries of their residual envelopes, and with different optical depths of their CSEs. This depends not only on their main-sequence mass, but also on the exact moment of mass exhaustion in the envelope during the thermal pulse cycle. The departure from the AGB is marked by the cessation of large amplitude variability and by a remnant CSE, which is detached. The stars move for a brief period (few 10^3 years) into the extremely red parts of the IRAS color-color diagram ([25–12]>0.0 in Fig. 2). Candidates are the 'non-variable OH/IR stars', in which the outermost OH maser zone is still undisturbed, but the H_2O masers respond to decreasing densities in the inner CSE (Engels 2002).

5. Post-AGB stars

5.1. Evolution

As shown in Figure 6 the OH/IR star like heavily obscured SED at the tip of the AGB will change on short timescales (≈ 500 years for

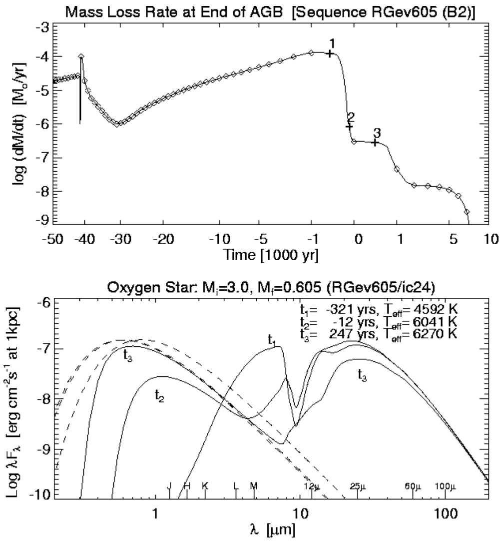

Fig. 6. Development of the mass loss rate after the last thermal pulse (top) and development of a double-peaked spectral energy distribution (bottom) in response to the drop of the mass loss rate between time stamps t_1 and t_3 (from Steffen et al. (1998)).

the 3 $M_{\odot}$ model of Steffen et al. (1998)) to a double-peaked distribution, in which the central star shines through the now diluted CSE. Parallel to the mass loss reduction, the star (the former core) now begins to contract and heat up. In the HRD (Fig. 1), it develops almost horizontally with constant luminosity to higher temperatures. If the temperature reaches 25 000 K the radiation is able to ionize the remnant CSE, well visible then as planetary nebula. Surprisingly, the post-AGB mass loss rate was not found to be zero albeit small (≈ 10^{-8} $M_{\odot}$). Furthermore the winds speeds are much higher than on the AGB reaching 10^3 kms^{-1}.

The time scales that models predict for the post-AGB phase range between 10^1 and 10^5 years depending inversely on the core mass, the treatment of the mass loss reduction process, and the mass loss history on the AGB (Blöcker 1995b). This implies that not all post-AGB stars will eventually become a planetary nebula. For low core masses the remnant CSEs might have dissipated before the stars are able to ionize the shell. For high core masses the temperature rise is so fast that the CSEs may still be opaque and emission from the ionized inner rim is trapped.

5.2. Observational characteristics

Considerable numbers of post-AGB stars were discovered using the IRAS All-Sky Survey to search for optical bright objects with strong mid-infrared excesses, e.g. stars with a double-peaked SED. Other searches focused on the red parts of the IRAS color color diagram, providing optically fainter post-AGB stars. A recent compilation contained 220 post-AGB stars and candidates (see Szczerba et al. in Szczerba & Górny (2001)). Statistically well defined samples are still lacking and new approaches to find new post-AGB stars are clearly warranted (Richards, these proceedings). Optical spectroscopy of post-AGB stars demonstrated that in accordance with the wide range of temperatures covered by the evolutionary tracks, all spectral types between B and K are present. Although lines of elements dredged-up during the AGB phase are detected, the chemical composition of the photospheres show a larger diversity as anticipated. The phase of the thermal pulse cycle when the star leaves the AGB may determine the chemical composition of the remaining envelope. But also the membership in a binary system seem to have more influence on observable properties than on the AGB, where only a few members in binary systems are known.

5.3. Mass loss and nebula shapes

Planetary nebulae and protoplanetary nebulae (PPN) show a large diversity of morphologies (Balick & Frank 2002). The most remarkable structural change, even for many very young PPN, is the loss of the radial symmetry prevalent for the mass loss on the AGB. A case in point is the Egg nebula (Fig. 7), which displays a bipolar nebula morphology, created by polar outflows originating from the center of an optically thick dusty disk. The nebula is surrounded by spherically symmetric concentric arcs, which evidently are associated with the remnant AGB shell. The gaps between the arcs infer modulations of the AGB mass loss rates on time scales of a few hundred years, which neither fit to the thermal pulse nor to the envelope pulsation time scales.

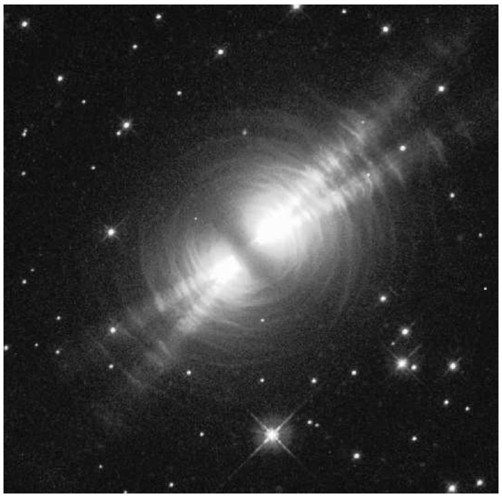

Fig. 7. Proto-Planetary Nebula AFGL 2688 (Egg Nebula). Credit: NASA and The Hubble Heritage Team (STScI/AURA)

The velocities of the bipolar (sometimes even multipolar) outflows have been mapped in about a dozen PPN in CO or in the H_2O or OH masers revealing velocities up to 10^3 kms^{-1}. The time scales implied for the age of these outflows are several hundred to a few thousand years, implying that the departure from the AGB happened only recently (see also Gomez, these proceedings). After having passed the planetary nebula stage, stars descend the white dwarf cooling track. However, some may experience a very late thermal pulse bringing them back to the AGB ('born-again AGB stars'). One case is Sakurai's object (V4334 Sgr) evolving with a fascinating pace on the timescale of years across the HRD (Eyres, these proceedings).

Research on post-AGB stars is a lively field and we still lack a coherent picture, matching evolutionary theories with the bewildering diversity of post-AGB star types. The accumulation of knowledge proceeds fast and is reflected by recent publications of Kwok (2000), Szczerba & Górny (2001), Van Winckel (2003) and Waelkens & Waters (2004).

6. Brief outlook

Research on AGB and post-AGB stars has advanced strongly in the last 25 years, beginning with the discovery of thousands of new objects by IRAS. Key open questions encompass the primary mass loss mechanism, the influence of thermal pulses on observational properties and the origin for the transition of radial symmetric mass loss on the AGB to axi- or point-symmetric high-velocity outflows in the post-AGB phase. The understanding of the key physics for the mass loss process is of great importance, because both the AGB evolution models as well as the models to synthesize the AGB population in foreign galaxies still rely on uncertain empirical mass loss laws. With the advent of upcoming new instrumentation, we expect a much better understanding of the processes near the photosphere. Monitoring will be mandatory in many cases to describe correctly the effects of pulsation. The ambiguities due to uncertain distances will be overcome by intensifying the study of AGB populations in the Magellanic Clouds and extending studies towards other galaxies of the Local Group. However, due to the inherent variability of the stars, small sized telescopes with robotic observing equipment will also be able to contribute substantially to modern AGB research.

References

Balick, B., & Frank, A. 2002, *Shapes and Shaping of Planetary Neb.*, ARA&A 40, 439

Bedijn, P.J. 1987, A&A, 186, 136

Blöcker, T. 1995a, A&A, 297, 727

Blöcker, T. 1995b, A&A, 299, 755

Blommaert, J. 2005, in *ISO science legacy*, Springer (in press)

Cohen , R. J. 1989, *Compact maser sources*, Rep. Prog. Phys., 52, 881

Diamond, P. J., Kemball, A. J. 2003, ApJ, 599, 1372

Elitzur, M. 1992a, *Astronomical Masers*, ARA&A, 30, 75

Elitzur, M. 1992b, *Astronomical Masers*, Kluwer Academic Publishers

Engels, D., Kreysa, E., Schultz, G. V., & Sherwood, W. A. 1983, A&A, 124, 123

Engels, D. 2002, A&A, 388, 252

Groenewegen M. A. T., & Marigo, P. 2004, in Habing & Olofsson (2004), p. 105-148

Habing, H. J., 1996, *Circumstellar envelopes and Asymptotic Giant Branch stars*, A&ARA, 7, 97

Habing, H. J., & Olofsson, H. 2004, *Asymptotic Giant Branch Stars*, Springer-Verlag

Koester, D. & Reimers, D. 1996, A&A 318, 810

Kwok, S. 2000, *The Origin and Evolution of Planetary Nebulae*, Cambridge Univ. Press

Lattanzio, J. C., & Wood, P. R., 2004, in Habing & Olofsson (2004), p. 23–104

Kharchenko, N., Kilpio, E., Malkov, O., Schilbach E. 2002, A&A, 384, 925

Lewis, B.M. 1994, ApJS, 93, 549

Molster, F., & Kemper, C. 2005, in *ISO science legacy*, Springer (in press)

Olivier, E. A., Whitelock, P., & Marang, F. 2001, MNRAS, 326, 490

Reid, M. J. & Goldstone, J. E. 2002, ApJ, 568, 931

Samus, N. N., Durlevich, O. V., et al. 2004, GCVS4.2, Moscow

Sylvester R. J., Kemper, F., Barlow, M. J., et al. A&A, 352, 587

Szczerba, R., & Górny, S. K. (Eds.) 2001, *Post-AGB objects as a phase of stellar evolution*, Kluwer Academic Publishers

Steffen, M., Szczerba, R., Schönberner, D. 1998, A&A 337, 149

Stephenson, C. B. 1989, *A general catalog of cool galactic carbon stars*, 2nd Edition

van der Veen, W.E.C.J., & Habing, H.J. 1988, A&A, 194, 125

Van Winckel, H. 2003, *Post-AGB stars*, ARA&A 41, 391

Vassiliadis, E., & Wood, P.R. 1993, ApJ, 413, 641

Waelkens, C., & Waters, R. B. F. M. 2004, in Habing & Olofsson (2004), p. 519–554

Wallerstein, G., & Knapp, G. R. 1998, ARA&A, 36, 369

Willson, L. A. 2000, ARA&A, 38, 573